J Mater Sci (2018) 53:12641–12649

Polymers

A sustainable adsorbent for phosphate removal: modifying multi-walled carbon nanotubes with chitosan

Yimin Huang[1,2,3], Xinqing Lee[1,*], Matteo Grattieri[3], Florika C. Macazo[3], Rong Cai[3], and Shelley D. Minteer[3,*]

[1] State Key Laboratory of Environmental Geochemistry, Institute of Geochemistry, Chinese Academy of Science, Guiyang 550081, Guizhou, China
[2] University of Chinese Academy of Sciences, Beijing 100049, China
[3] Departments of Chemistry and Materials Science and Engineering, University of Utah, 315 S 1400 E, Salt Lake City, UT 84112, USA

Received: 28 April 2018
Accepted: 23 May 2018
Published online: 5 June 2018

ABSTRACT

Phosphorus, a major culprit for eutrophication of aquatic environments, is dissolved in water primarily in the form of phosphate; hence, it is difficult to remove, and different materials are being investigated, aiming at high removal capabilities. Meanwhile, recovery capability must also be considered, since phosphorus present in wastewater may serve as a potential alternative resource for the mineral phosphorus. Carbon nanotubes are promising for the treatment of phosphate pollution; however, studies about their removal potential are limited. Herein, multi-walled carbon nanotubes were modified with chitosan through simply cross-linking to obtain a novel adsorbent for phosphate removal. Our data show that a maximum adsorption as high as 36.1 ± 0.3 mg P g^{-1} was achieved in 30 min at pH 3 and 293 K. The adsorption capacity of the composite (chitosan/multi-walled carbon nanotubes) could be maintained at 94–98% even after 5 adsorption–desorption cycles. An exothermic process was obtained, according to the Freundlich isotherm model. Based on the reported performance, the composite has a great advantage compared with other novel adsorbents for phosphate removal, indicating that the composite is a highly potential material to treat phosphorus-induced eutrophication of water bodies.

Introduction

In aquatic environments phosphorus represents an essential macronutrient [1]. However, when exceeding 0.02 mg L^{-1} in water, it induces the problem of eutrophication in favorable conditions, deteriorating the water quality through oxygen depletion, light transmission reduction, and algae blooms [2]. *P* normally exists in the environment as phosphate [3], which is particularly soluble, and thus, is difficult to remove. The different approaches used to remove

Address correspondence to E-mail: lee@mail.gyig.ac.cn; minteer@chem.utah.edu

https://doi.org/10.1007/s10853-018-2494-y

phosphate from aqueous solution are characterized by high costs [4], such as electrocoagulation, biological method, ion exchange, chemical precipitation, membrane process, and adsorption [5]. In the USA alone, about $44.5 billion are required to lower the pollutant to the acceptable level (0.1 mg L^{-1}) [6]. Furthermore, it has to be noted that using conventional technologies it is difficult to recover and utilize trace phosphate [7], and thus, there is a need for new strategies to remove phosphate from aquatic environments [1]. Adsorption is an appealing alternative as it allows simple and low-cost operation. Additionally, if the right adsorbent is used, there is the potential for phosphate recovery from contaminated water [7]. Carbon nanotubes (CNTs) are a relatively new member of materials utilized for adsorption processes. They are characterized by nanometer-scale diameter sizes, large surface area, high mechanical strength, and have an outstanding electrical conductivity, making them an attractive material for adsorption of metallic and organic pollutants in the aquatic environments [8–13]. To date, the use of CNT for phosphate removal has been reported only in few studies, which showed good adsorption capability (15.4 mg P g^{-1}), thus making CNT a promising substitute adsorbent for treating wastewater contaminated with inorganic phosphate [14]. However, phosphate adsorption potential of CNT, together with adsorption mechanisms, is not fully known.

Chitosan is an environmentally friendly low-cost biopolymer, characterized by a high amount of amino and hydroxyl groups, which are particularly important when aiming to remove negatively charged pollutants from aqueous solutions. Some research demonstrated that when chitosan is loaded onto multi-walled CNTs, the resulting composite shows high adsorption capability with good reusability for heavy metal removal [15]. To the best of the authors' knowledge, chitosan-modified multi-walled carbon nanotubes have not been tried for the purpose of phosphate removal. Therefore, we believe that the phosphate removal potential of chitosan/multi-walled carbon nanotubes (chitosan/MWCNTs) is worth exploring because of its excellent performance. Herein, we report a novel adsorbent (chitosan/MWCNTs) for phosphorus removal, aiming to explore the potential ability of CNTs for effective phosphate sorption and recycling. Our data show that the reaction time needed for phosphate adsorption was considerably shortened (only 30 min), demonstrating the effective removal of phosphate from aqueous solutions. Additionally, phosphate could by released with a desorption process, showing excellent regeneration properties.

Materials and methods

MWCNTs (30–50 nm in diameter) utilized for this study were purchased from Cheap Tubes Co. Ltd. (Cambridgeport, VT). All other reagents were of analytical grade and were obtained from Sigma-Aldrich (St. Louis, MO). Ultrapure water (18.25 MΩ cm) was used to prepare all the solutions.

Preparation and characterization of chitosan/MWCNTs composite

An established method [15] was followed to prepare the chitosan/MWCNTs composite. Briefly, MWCNTs was added in a 2% (v/v) acetic acid solution of chitosan and stirred for 15 min at 40 °C. Then, 0.4 mL of glutaraldehyde was injected into the mixture and stirred for 30 min. After this operation, 1L of water and 120 mL of 0.10 M NaOH were added and stirred for another 30 min. The supernatant solution was removed, and the remaining sample was dried at 80 °C in an oven (Isotemp® Vacuum Oven Model 282A). The surface chemistries of MWCNTs and chitosan/MWCNTs were analyzed by X-ray photoelectron spectroscopy (XPS, Kratos Axis Ultra DLD system).

Batch studies

We investigated the effect of pH on adsorption process, adsorption kinetics and isotherms. In all batch studies, 0.05 g adsorbent was added in 250-ml Erlenmeyer flask with 50 ml phosphate solution.

pH of the solution was modified between 2.0 and 7.0 to investigate its effect on phosphate adsorption by chitosan/MWCNTs and MWCNTs. The following experiments were investigated at the optimal pH (pH 3). The pH of solution was changed with 0.1 M HCl and 0.1 M NaOH solution.

Adsorption kinetics were measured with different concentrations (25, 50, 100 mg P L^{-1}) and time (5, 10, 20, 30, 60, 120 min). Adsorption isotherms were determined at three temperatures (293, 303, and 313 K) and different initial phosphate concentrations (from 25 to 200 mg P L^{-1}).

Samples were filtered by 0.45-μm fiber membranes. UV–Vis spectroscopy (Evolution 260 Bio UV-Vis spectrophotometer, Thermo Scientific) was utilized to determine phosphate concentration in the filtrate, at a wavelength of 710 nm. The adsorbed phosphate per unit mass of the adsorbent was then calculated using the following equation:

$$q_e = \frac{V(C_0 - C_e)}{m}, \quad (1)$$

where q_e is the adsorption capacity (mg P g^{-1}), C_0 and C_e indicate initial and equilibrium concentrations of phosphate (mg P L^{-1}), respectively, V is the total volume (L) of solution, and m indicates weight (g) of adsorbent.

Desorption experiments

Desorption of phosphate from chitosan/MWCNTs was performed using a solution of 0.1 M NaOH. 0.5 g of chitosan/MWCNTs was added to 0.5 L phosphate solution (200 mg P L^{-1}). The solution was shaken for 2 h at 303 K to allow the adsorption of phosphate. The obtained mixture was then filtered using a Buchner funnel and washed with ultrapure water. 0.5 L of 0.1 M NaOH was added and was shaken for 2 h at 303 K. This step allowed to remove phosphate from the composite. Finally, the mixture was filtered one more time using the Buchner funnel and washed with ultrapure water. The adsorption capacity for phosphate was then calculated according to Eq. 1.

Results and discussion

Characterization of adsorbent composites

Appearance of a small *N* 1s peak at 400.3 eV (Fig. 1 right, red curve) confirmed the successful modification of MWCNTs with chitosan. Focusing on the spectra obtained for the composite after adsorption (right insert, red curve), and desorption of phosphate (right insert, blue curve), it can be noticed that a *P* 2*p* peak (~ 133 eV) appeared and disappeared, respectively. Thus, the composite was able to perform an efficient adsorption of phosphate followed by its complete desorption. Additionally, the *N* 1s peak indicates that the amino group remained also after the desorption process, remarking the excellent reusability of the composite.

The N 1s core-level spectrum obtained for the composite (Fig. 2) was deconvoluted into two peaks with binding energies of about 399.9 and 402.5 eV. The peaks were attributed to the benzenoid nitrogen (NH-) present in the Py ring and to the positively charged nitrogen species (NH^+-), respectively [16]. The percent of NH^+- after adsorption is significantly higher than that prior to performing the adsorption

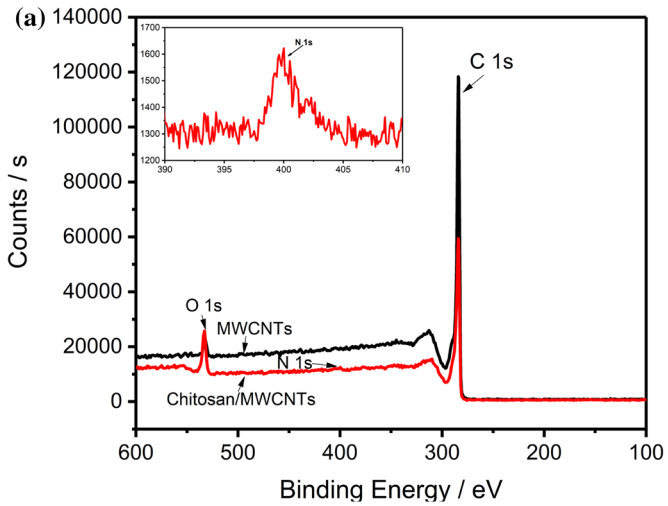

Figure 1 XPS spectra for the adsorbent composite obtained before (black) and after modification with chitosan (red), with a zoom (inset) of the *N* 1s peak for the modified composite (**a**).

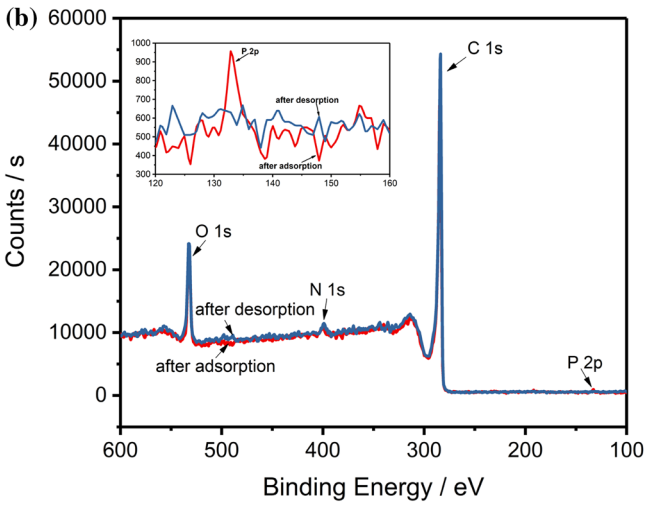

Comparative XPS spectra after adsorption (red) and after desorption of phosphate (blue) for the modified composite, with a zoom of the *P* 2*p* peaks (inset) for the P adsorbed (**b**).

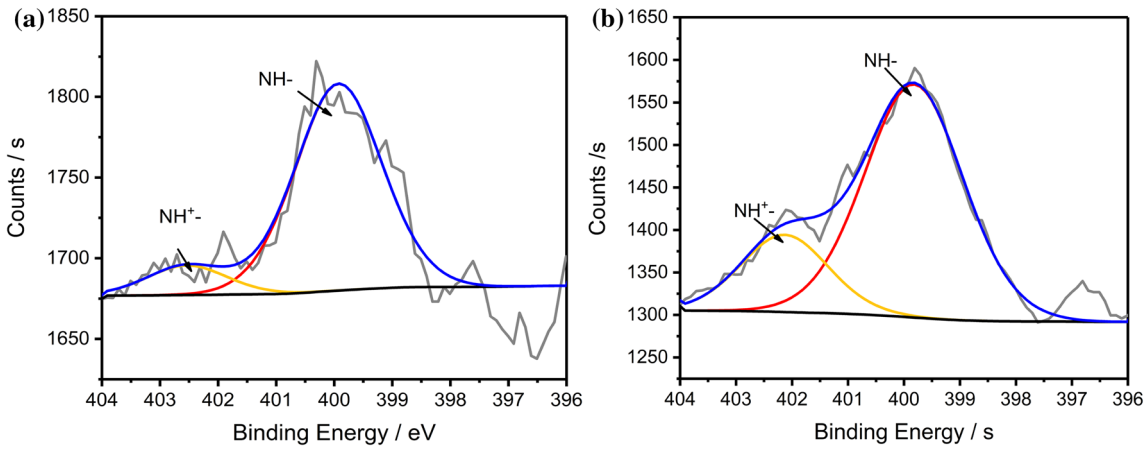

Figure 2 N 1s XPS spectra of the composite before (**a**) and after adsorption (**b**).

(Fig. 2), indicating a physical electrostatic adsorption between anionic phosphate and chitosan/MWCNTs.

pH influence on adsorption process

pH of the solution to be treated can both influence the surface charge of the adsorbent and dictate the form of the adsorbate. Accordingly, the effect of pH on the adsorption process was selected as the first parameter to be investigated in this study. Unmodified MWCNTs showed no adsorption for phosphate (Fig. 3, red). Conversely, chitosan-modified MWCNTs have good adsorption capability for phosphate (Fig. 3, blue), with a maximum adsorption at pH 3 (19.4 mg g^{-1}) that gradually decreased as pH increased.

Based on the presented results, three reaction mechanisms can be suggested. First, phosphate is present in the non-ionic form, H_3PO_4 at pH 2, whereas it exists as $H_2PO_4^-$, HPO_4^{2-}, and PO_4^{3-} in the pH range of 2–7, 7–12.5, and 12.5, respectively [17], and the adsorption of $H_2PO_4^-$ is easier than that of HPO_4^{2-} [17]. Second, the surface charge of chitosan/MWCNTs is positive when the pH < pH_{pzc}, resulting in a stronger electrostatic adsorption of the anionic phosphate on the surface. Moreover, phosphate anion and OH − compete for the adsorption in alkaline conditions, resulting in a decrease in phosphate removal as pH increased [18].

Adsorption kinetics and modeling

As indicated in Fig. 4, contact time significantly affected the adsorption process, showing that the removal process was a series of fast processes. More

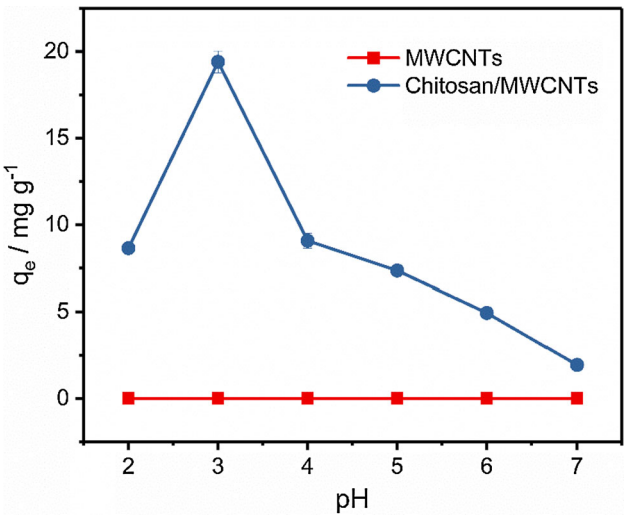

Figure 3 Phosphate adsorption on MWCNTs (red) and chitosan/MWCNTs composite (blue) at different pH. All the experiments were performed at 303 K, with an adsorbent dose of 0.05 g in 50 mL of 100 mg P L^{-1} solution.

than 90% of the adsorption occurs in the first 20 min, and equilibriums were reached at 30 min at concentrations of 25, 50, and 100 mg P L^{-1}(Fig. 4), a considerably shorter time compared to other reports (8 h [7], 24 h [19], five or more days [20]).

Equations of pseudo-first-order and pseudo-second-order rate were utilized to calculate relevant kinetic parameters [21–23]:

$$q_t = q_e(1 - \exp(-k_1 t)) \quad (2)$$

$$\frac{t}{q_t} = \frac{1}{K_2 q_e^2} + \frac{t}{q_e}, \quad (3)$$

where q_t (mg P g^{-1}) and q_e (mg P g^{-1}) indicate the adsorption capacities of ions at time t (min) and

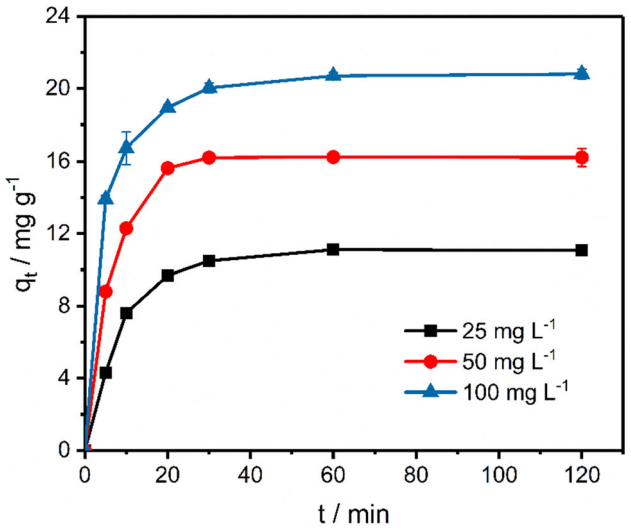

Figure 4 Adsorption–time graphs at 303 K for phosphate concentrations of 25 mg L^{-1} (black), 50 mg L^{-1} (red), and 100 mg L^{-1} (blue). The adsorbent dose was 0.05 g in a 50 mL solution (pH = 3.0).

equilibrium time (min), respectively. k_1 (min^{-1}) and k_2 (g mg^{-1} min^{-1}) are the pseudo-first-order and pseudo-second-order rate constants, respectively.

Table S1 reports the obtained values for both models. It can be seen that the q_e^{cal} values of the pseudo-first-order kinetics model were close to experimental q_e^{exp}, although both models gave R^2 values higher than 0.9. Accordingly, the pseudo-first-order kinetics model is considered more appropriate for the adsorption process. Since a physisorption process is assumed as the rate-limiting step for the pseudo-first-order kinetics, it can be assumed that a physical process controls the adsorption of phosphate by chitosan/MWCNTs. The k_2 value was 7.55×10^{-3}, 3.65×10^{-3}, and $2{,}24 \times 10^{-3}$ g mg^{-1} min^{-1} for initial phosphate concentrations of 25 mg L^{-1}, 50 mg L^{-1}, and 100 mg L^{-1}, indicating the adsorption rate at low concentration was faster than high concentration. In conclusion, the chitosan/MWCNTs is a favorable adsorbent for adsorption of low concentration phosphate [24], which is an advantage for the treatment of real wastewater solutions.

A novel quaternized chitosan–melamine–glutaraldehyde resin was reported to have a great phosphate adsorption capacity (112.5 mg g^{-1}) by Appunni Sowmya et al. [25]. However, the adsorption rate was higher at 160 mg L^{-1} rather than at 100 mg L^{-1}, indicating that the adsorbent worked better at high concentration of phosphate, which is less common in real water sample. Meanwhile, the adsorption rate of the composite is significantly slower compared to the chitosan/MWCNTs reported here at phosphate concentration of 100 mg L^{-1} ($5.70 \times 10^{-4} < 2.24 \times 10^{-3}$ g mg^{-1} min^{-1}). Rajeswari et al. [26] synthesized chitosan–polymer composites for phosphate removal with maximum phosphate adsorption of 98.8 mg $g^{-1,}$ obtaining an increase in the adsorption rate with decreased phosphate concentration as for chitosan/MWCNTs. However, the adsorption rate of the chitosan–polymer composites remained slower than that of chitosan/MWCNTs even at phosphate concentration of 50 mg L^{-1} ($5.20 \times 10^{-4} < 3.65 \times 10^{-3}$ g mg^{-1} min^{-1}).

Considering the results discussed above it remains clear that the adsorption capability of chitosan/MWCNTs will still have to be improved; however, its advantageous adsorption rate makes it a promising adsorbent for the treatment of phosphate pollution.

Identification of the adsorption process is essential for developing an optimal adsorption system, as well as for prediction of the rate-limiting step [27]. Adsorption dynamics included three consecutive steps. The first step is boundary diffusion, where the adsorbate diffused on the adsorbent exterior surface. Intraparticle diffusion into the pores of the adsorbent represents the second step. In the third step adsorbate was adsorbed into the interior site of the adsorbent. Weber Morris intraparticle diffusion model (Eq. 4) was used to investigate the rate-limiting step of phosphate adsorption. If plotting q_t versus $t^{0.5}$ a straight line is obtained, passing through the origin, intraparticle diffusion is the sole rate-controlling step [24]. In contrast, the adsorption process was controlled by two or more steps [28].

$$q_t = k_p t^{0.5} + C, \tag{4}$$

where q_t is the adsorption amount at time t (mg g^{-1}), k_p is the intraparticle diffusion constant (mg g^{-1} $min^{-1/2}$), and C is the intercept (mg g^{-1}).

In this study, the multi-linearity of phosphate adsorption on the composite (Fig. 5) suggested that the whole adsorption process can be divided into three steps. Specifically, the slope of each linear segment in the plot determines the rate of adsorption, where a higher slope indicates a faster adsorption process [27]. The k_1 of three phosphate concentration was significantly higher than k_2 and k_3, suggesting

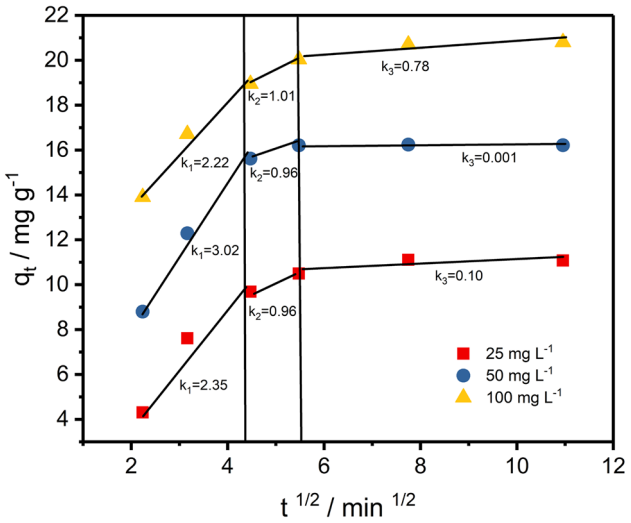

Figure 5 Intraparticle diffusion model for phosphate adsorption onto chitosan/MWCNTs.

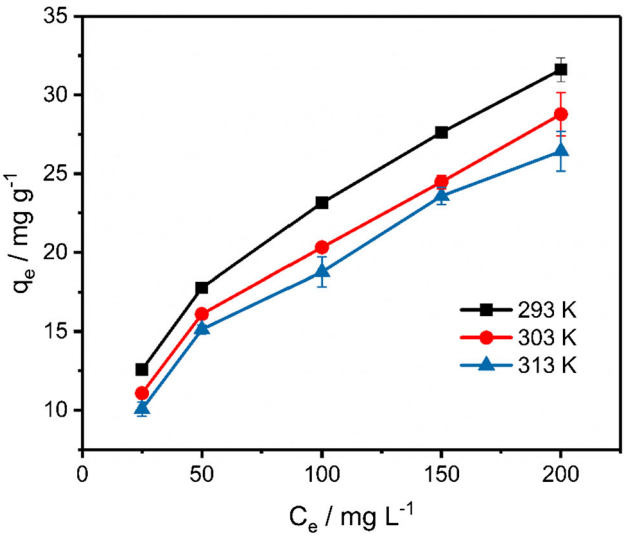

Figure 6 Adsorption of phosphate by chitosan/MWCNTs composite at 293 K (black), 303 K (red), and 313 K (blue). The adsorbent dose was 0.05 g in a 50 mL (pH = 3.0) solution. Phosphate concentrations were increased from 25 to 200 mg P L^{-1}.

that boundary diffusion was the dominating step, followed by intraparticle diffusion.

Adsorption isotherms

Adsorption isotherms could be constructed based on the results obtained at different temperatures and equilibrium concentrations of the adsorbate and were analyzed using the Langmuir and Freundlich isotherm models [29]:

$$\frac{C_e}{q_e} = \frac{1}{K_L q_m} + \frac{1}{q_m} C_e \quad (5)$$

$$\ln q_e = \ln K_F + \frac{1}{n} \ln C_e, \quad (6)$$

where q_m indicates the maximum adsorption (mg g^{-1}), K_L is the adsorption equilibrium constant (L mg^{-1}), C_e is the equilibrium concentration of substrates in solution (mg L^{-1}), K_F is a constant representing adsorption capacity, and n is a constant depicting the adsorption intensity.

It is shown in Fig. 6 that the adsorption capacity of chitosan/MWCNTs gradually increased with increasing concentration of phosphate. Meanwhile, increasing the temperature resulted in decreased adsorption capacity of chitosan/MWCNTs. Table S2 summarizes the parameters calculated applying Langmuir and Freundlich models to the adsorption data obtained for different temperatures. Maximum adsorption capacity was calculated to be 36.1 ± 0.3–31.3 ± 0.7 mg P g^{-1} in the investigated temperature range. As indicated, both the correlation coefficients (R^2) of Langmuir and Freundlich models are > 0.9, suggesting that the adsorption abides well by the two models. However, experimental results are better fitted by the Freundlich isotherm model, suggesting that phosphate is mainly adsorbed on the surface of the adsorbent in a multilayer coverage manner. Freundlich isotherm model indicates a favorable physical process when $(1/n)$ is close to zero, as well as if n is higher than unity. Additionally, values of $2 \le n \le 10$, $1 \le n < 2$, and $n < 1$ represent an easy adsorption, a moderate adsorption, and a difficult adsorption, respectively [30]. The obtained values of 0.35–0.38 for $1/n$, and 2.63–2.86 for n, shown in Table S2, confirm that the adsorption process is physical and favorable.

Different studies that focus on the synthesis of novel adsorbent can be found in the literature, due to urgency of phosphate pollution treatment. Among remarkable reports, Yoon et al. [19] synthesized magnetic iron oxide nanoparticles, which reached adsorption equilibrium at 24 h with the maximum sorption capacity of 5.03 mg P g^{-1}. Rashid et al. [31] demonstrate that humic acid-coated magnetite nanoparticles allow a fast and effective removal of phosphate, achieving a maximum adsorption capacity of 28.9 mg P g^{-1}. Qin et al. [1] reported zirconium oxide as a novel adsorbent that can remove

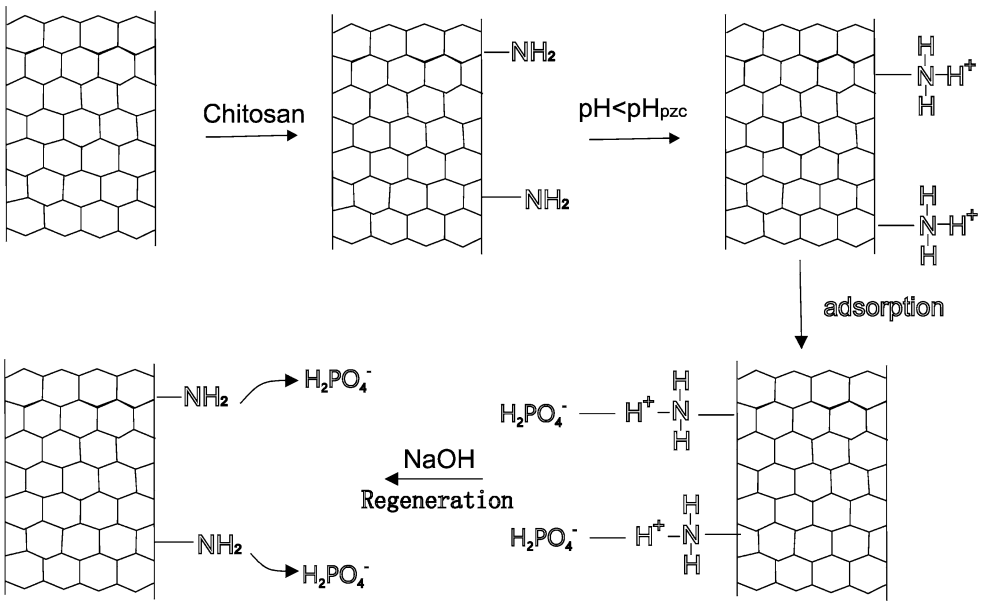

Figure 7 Preparation route, adsorption, and regeneration mechanism of chitosan/MWCNTs.

phosphate with maximum adsorption capacity of 1.21 mg P g^{-1}. Beyond these, adsorption capabilities of other novel adsorbents are summarized in Table S3. It can be easily noticed that the adsorption capability of the composite presented in this work is higher than many other phosphate adsorption systems recently reported in the literature. Though the adsorption capability of the presented composite is lower than that in some reports [7, 18], its extremely simple modification method, significantly shorter equilibrium time, and excellent reusability (*vide infra*) make it an attractive candidate to deal with phosphate pollution in aquatic environments.

Thermodynamic of the adsorption process

Thermodynamic parameters of phosphate adsorption were studied by performing experiments at 293, 303, and 313 K. A negative value of ΔH° (− 7.51 kJ mol^{-1}) indicates an exothermic adsorption; thus, it was reduced at increasing temperatures. Negative values of ΔG° (− 16.77, − 17.00, and − 17.41 kJ mol^{-1}) indicate that the adsorption was spontaneous. Finally, a positive value of ΔS° (0.032) implies increased randomness at the solid–solution interface, which helped the adsorption of phosphate on the surface of chitosan/MWCNTs.

Regeneration studies

In order to be applied for the treatment of real water samples, an excellent adsorbent should possess both a high adsorption capacity and excellent reusability to reduce the overall cost. For the specific case of phosphate removal, the desorption capability of the adsorbent is of utmost importance since phosphate is considered a "non-renewable resource," and it may be depleted in less than a century due to world growing demands [7]. Here, the reusability of our chitosan/MWCNTs composite was investigated in five adsorption–desorption cycles. The calculated adsorption capacities indicate that the composite maintained good adsorption performance up to the fifth cycle (∼ 94 to 98%). Furthermore, XPS result indicated a percentage of phosphorus of ∼ 3% after adsorption of phosphate on the surface of the chitosan/MWCNTs composite; however, after desorption, the percentage of *P* decreased from ∼ 3 to ∼ 0%. This result confirms that phosphate was completely released from the surface of chitosan/MWCNTs and the composite possess excellent reusability and potential for phosphate recovery.

Proposed mechanism for phosphate adsorption

As previously discussed, the adsorption of phosphoric ions was considerably influenced by the pH, due to electrostatic attraction between adsorbent and

adsorbate. A schematic of the mechanism is shown in Fig. 7. Amine groups of chitosan largely take part in the overall adsorption process, where they get protonated at low pH, thus imparting a significant positive charge on the surface of the adsorbent and thereby aiding in the effective adsorption of negatively charged phosphate species. This process is supported by the *N* 1s XPS spectra obtained for the chitosan/MWCNTs composite. Moreover, NaOH can break the electrostatic attraction between chitosan/MWCNTs and phosphate, thus allowing for the complete release of phosphate and the recovery of adsorption site after desorption, suggesting an electrostatic adsorption mechanism for phosphate removal by chitosan/MWCNTs.

Conclusions

The reported adsorbent for phosphate provides powerful proof for phosphate removal potential using carbon nanotubes. The study indicated that the developed composite showed a good phosphate adsorption capability in aqueous solutions, as high as 36.10 mg P g^{-1} at pH 3 and 293 K. The maximum adsorption was reached in only 30 min with a spontaneous and exothermic process, a much shorter time compared with other reports. Additionally, the composites showed excellent reusability, retaining 94–98% of the adsorption capacity after 5 adsorption–desorption cycles. The composite showed a remarkable performance compared to other novel adsorbents reported, further confirming its great potential for phosphate removal and recycling. Optimization of the effective pH range for application of the composites will be an important aspect to be considered in future studies, as well as the use of different functional groups.

Acknowledgements

This work was supported by the State Scholarship Fund sponsored by the China Scholarship Council (Y. H.), National Natural Science Foundation of China (U1612441), Sino-Israeli Intergovernmental Scientific and Technological Cooperation Project (2015DFG92 450), and the 2014 Cooperative Project Between the Chinese Academy of Sciences and the Xinjiang Autonomous Region (X.L.). The authors would also like to thank the United States National Science Foundation, under award number 1561427 (M.G., F.C.M., and S.D.M.), for financial support.

Compliance with ethical standards

Conflict of interest The authors declare that they have no conflict of interest.

Electronic supplementary material: The online version of this article (https://doi.org/10.1007/s10853-018-2494-y) contains supplementary material, which is available to authorized users.

References

[1] Qin K, Li F, Xu S, Wang T, Liu C (2017) Sequential removal of phosphate and cesium by using zirconium oxide: a demonstration of designing sustainable adsorbents for green water treatment. Chem Eng J 322:275–280

[2] Khalil AM, Eljamal O, Amen TW, Sugihara Y, Matsunaga N (2017) Optimized nano-scale zero-valent iron supported on treated activated carbon for enhanced nitrate and phosphate removal from water. Chem Eng J 309:349–365

[3] Vaccari DA (2009) Phosphorus: a looming crisis. Sci Am 300:54–59

[4] Oladoja NA, Ahmad AL, Adesina OA, Adelagun ROA (2012) Low-cost biogenic waste for phosphate capture from aqueous system. Chem Eng J 209:170–179. https://doi.org/10.1016/j.cej.2012.07.125

[5] Liu Q, Hu P, Wang J, Zhang L, Huang R (2016) Phosphate adsorption from aqueous solutions by Zirconium (IV) loaded cross-linked chitosan particles. J Taiwan Inst Chem Eng 59:311–319

[6] Ramasahayam SK, Guzman L, Gunawan G, Viswanathan T (2014) A comprehensive review of phosphorus removal technologies and processes. J Macromol Sci A 51:538–545

[7] Qiu H, Liang C, Yu J, Zhang Q, Song M, Chen F (2017) Preferable phosphate sequestration by nano-La (III)(hydr) oxides modified wheat straw with excellent properties in regeneration. Chem Eng J 315:345

[8] Grattieri M, Shivel ND, Sifat I, Bestetti M, Minteer SD (2017) Sustainable hypersaline microbial fuel cells: inexpensive recyclable polymer supports for carbon nanotube conductive paint anodes. Chemsuschem 10:2053–2058

[9] Minteer SD, Liaw BY, Cooney MJ (2007) Enzyme-based biofuel cells. Curr Opin Biotechnol 18:228–234

[10] Bandodkar AJ, Wang J (2016) Wearable biofuel cells: a review. Electroanalysis 28:1188–1200

[11] Macazo FC, Hickey DP, Abdellaoui S, Sigman MS, Minteer SD (2017) Polymer-immobilized, hybrid multi-catalyst architecture for enhanced electrochemical oxidation of glycerol. Chem Commun 53:10310–10313. https://doi.org/10.1039/C7CC05724E

[12] Pillay K, Cukrowska EM, Coville NJ (2009) Multi-walled carbon nanotubes as adsorbents for the removal of parts per billion levels of hexavalent chromium from aqueous solution. J Hazard Mater 166:1067–1075. https://doi.org/10.1016/j.jhazmat.2008.12.011

[13] Kumar ASK, Jiang S-J, Tseng W-L (2015) Effective adsorption of chromium (VI)/Cr (III) from aqueous solution using ionic liquid functionalized multiwalled carbon nanotubes as a super sorbent. J. Mater. Chem. A 3:7044–7057

[14] Mahdavi S, Akhzari D (2016) The removal of phosphate from aqueous solutions using two nano-structures: copper oxide and carbon tubes. Clean Technol Environ Policy 18:817–827. https://doi.org/10.1007/s10098-015-1058-y

[15] Huang Y, Lee X, Macazo FC, Grattieri M, Cai R, Minteer SD (2018) Fast and efficient removal of chromium (VI) anionic species by a reusable chitosan-modified multi-walled carbon nanotube composite. Chem Eng J 339:259–267. https://doi.org/10.1016/j.cej.2018.01.133

[16] Bhaumik M, Agarwal S, Gupta VK, Maity A (2016) Enhanced removal of Cr (VI) from aqueous solutions using polypyrrole wrapped oxidized MWCNTs nanocomposites adsorbent. J Colloid Interface Sci 470:257–267

[17] Sowmya A, Meenakshi S (2013) An efficient and regenerable quaternary amine modified chitosan beads for the removal of nitrate and phosphate anions. J Environ Chem Eng 1:906–915

[18] Cui G, Liu M, Chen Y, Zhang W, Zhao J (2016) Synthesis of a ferric hydroxide-coated cellulose nanofiber hybrid for effective removal of phosphate from wastewater. Carbohyd Polym 154:40–47

[19] Yoon S-Y, Lee C-G, Park J-A et al (2014) Kinetic, equilibrium and thermodynamic studies for phosphate adsorption to magnetic iron oxide nanoparticles. Chem Eng J 236:341–347

[20] Lalley J, Han C, Mohan GR et al (2015) Phosphate removal using modified Bayoxide® E33 adsorption media. Environ Sci Water Res Technol 1:96–107

[21] Hu J, Chen C, Zhu X, Wang X (2009) Removal of chromium from aqueous solution by using oxidized multiwalled carbon nanotubes. J Hazard Mater 162:1542–1550. https://doi.org/10.1016/j.jhazmat.2008.06.058

[22] Ho YS, McKay G (1999) Pseudo-second order model for sorption processes. Process Biochem 34:451–465. https://doi.org/10.1016/S0032-9592(98)00112-5

[23] Wang J, Pan K, He Q, Cao B (2013) Polyacrylonitrile/polypyrrole core/shell nanofiber mat for the removal of hexavalent chromium from aqueous solution. J Hazard Mater 244:121–129. https://doi.org/10.1016/j.jhazmat.2012.11.020

[24] Lu J, Xu K, Yang J, Hao Y, Cheng F (2017) Nano iron oxide impregnated in chitosan bead as a highly efficient sorbent for Cr (VI) removal from water. Carbohyd Polym 173:28–36. https://doi.org/10.1016/j.carbpol.2017.05.070

[25] Sowmya A, Meenakshi S (2014) A novel quaternized chitosan–melamine–glutaraldehyde resin for the removal of nitrate and phosphate anions. Int J Biol Macromol 64:224–232. https://doi.org/10.1016/j.ijbiomac.2013.11.036

[26] Rajeswari A, Amalraj A, Pius A (2015) Removal of phosphate using chitosan–polymer composites. J Environ Chem Eng 3:2331–2341. https://doi.org/10.1016/j.jece.2015.08.022

[27] Bhaumik M, Agarwal S, Gupta VK, Maity A (2016) Enhanced removal of Cr (VI) from aqueous solutions using polypyrrole wrapped oxidized MWCNTs nanocomposites adsorbent. J Colloid Interface Sci 470:257–267. https://doi.org/10.1016/j.jcis.2016.02.054

[28] Boparai HK, Joseph M, O'Carroll DM (2011) Kinetics and thermodynamics of cadmium ion removal by adsorption onto nano zerovalent iron particles. J Hazard Mater 186:458–465. https://doi.org/10.1016/j.jhazmat.2010.11.029

[29] Jiang H, Chen P, Luo S, Tu X, Cao Q, Shu M (2013) Synthesis of novel nanocomposite Fe_3O_4/ZrO_2/chitosan and its application for removal of nitrate and phosphate. Appl Surf Sci 284:942–949. https://doi.org/10.1016/j.apsusc.2013.04.013

[30] Li C-J, Zhang S-S, Wang J-N, Liu T-Y (2014) Preparation of polyamides 6 (PA6)/Chitosan@ Fe_xO_y composite nanofibers by electrospinning and pyrolysis and their Cr (VI)-removal performance. Catal Today 224:94–103. https://doi.org/10.1016/j.cattod.2013.11.034

[31] Rashid M, Price NT, Pinilla MÁG, O'Shea KE (2017) Effective removal of phosphate from aqueous solution using humic acid coated magnetite nanoparticles. Water Res 123:353–360